



HAL
open science

Enzymatic Polycondensation of 1,6-Hexanediol and Diethyl Adipate: A Statistical Approach Predicting the Key-Parameters in Solution and in Bulk

Kifah Nasr, Julie Meimoun, Audrey Favrelle-Huret, Julien De Winter, Jean-Marie Raquez, Philippe Zinck

► **To cite this version:**

Kifah Nasr, Julie Meimoun, Audrey Favrelle-Huret, Julien De Winter, Jean-Marie Raquez, et al.. Enzymatic Polycondensation of 1,6-Hexanediol and Diethyl Adipate: A Statistical Approach Predicting the Key-Parameters in Solution and in Bulk. *Polymers*, 2020, 12 (9), pp.1907. 10.3390/polym12091907 . hal-03247367

HAL Id: hal-03247367

<https://hal.univ-lille.fr/hal-03247367v1>

Submitted on 3 Jun 2021

HAL is a multi-disciplinary open access archive for the deposit and dissemination of scientific research documents, whether they are published or not. The documents may come from teaching and research institutions in France or abroad, or from public or private research centers.

L'archive ouverte pluridisciplinaire **HAL**, est destinée au dépôt et à la diffusion de documents scientifiques de niveau recherche, publiés ou non, émanant des établissements d'enseignement et de recherche français ou étrangers, des laboratoires publics ou privés.

1 Article

2 Enzymatic polycondensation of 1,6-hexanediol and 3 diethyl adipate: A statistical approach predicting the 4 key-parameters in solution and in bulk

5 Kifah Nasr^{1,2}, Julie Meimoun¹, Audrey Favrelle-Huret¹, Julien De Winter³, Jean-Marie Raquez^{2*}
6 and Philippe Zinck^{1*}

7 ¹ Univ. Lille, CNRS, Centrale Lille, Univ. Artois, UMR 8181 –UCCS – Unité de Catalyse et Chimie du Solide,
8 F-59000 Lille, France; kifah.nasr@univ-lille.fr (K.N.); julie.meimoun@univ-lille.fr (J.M.); audrey.huret@univ-lille.fr (A.H.F.);

9
10 ² Laboratory of Polymeric and Composite Materials (LPCM), Center of Innovation and Research in Materials
11 and Polymers (CIRMAP), University of Mons, Place du Parc 23, 7000 Mons, Belgium; [jean-](mailto:jean-marie.raquez@umons.ac.be)
12 marie.raquez@umons.ac.be (J.M.R.)

13 ³ Center for Mass Spectrometry, Organic Synthesis and Mass Spectrometry Laboratory, University of Mons -
14 UMONS, 23 Place du Parc, 7000 Mons, Belgium; Julien.dewinter@umons.ac.be (J.D.)

15 * Correspondence: jean-marie.raquez@umons.ac.be; philippe.zinck@univ-lille.fr

16 Received: date; Accepted: date; Published: date

17 **Abstract:** Among the various catalysts that can be used for polycondensation reactions, enzymes
18 have been knowing a gain of interest since three decades, offering a green and eco-friendly platform
19 towards the sustainable design of renewable polyesters. However, limitations imposed by their
20 delicate nature, render them less addressed. As a case study, we compare herein bulk and solution
21 polycondensation of 1,6-hexanediol and diethyl adipate catalyzed by an immobilized lipase from
22 *Candida antarctica*. The influence of various parameters including time, temperature, enzyme
23 loading, and vacuum was assessed in the frame of a two-step polymerization with the help of
24 response surface methodology, a statistical technique that investigates relations between input and
25 output variables. Results in solution (diphenyl ether) and bulk conditions showed that 2 h reaction
26 time were enough to allow adequate oligomer growth for the first step conducted under
27 atmospheric pressure at 100°C. The number-average molecular weight (M_n) achieved varied
28 between 5,000 and 12,000 g.mol⁻¹ after a 24 h reaction and up to 18,500 g.mol⁻¹ after 48 h. The
29 statistical analysis showed that vacuum was the most influential factor affecting the M_n in diphenyl
30 ether. In sharp contrast, enzyme loading was found to be the most influential parameter in bulk
31 conditions. Recyclability in bulk conditions showed a constant M_n of the polyester over 3 cycles,
32 while a 17% decrease was noticed in solution. The following work finally introduced a statistical
33 approach that can adequately predict the M_n of poly(hexylene adipate) based on the choice of
34 parameter levels, providing a handy tool in the synthesis of polyesters where the control of
35 molecular weight is of importance.

36 **Keywords:** enzymatic polymerization; polycondensation; lipase; polyesters; response surface
37 methodology; recyclability

38

39 1. Introduction

40 Aliphatic and aromatic polyesters are more and more deserving a special attention as biobased
41 alternative to petropolymers due to their vast availability, large range of applications and to some of
42 them, their biodegradability [1–4]. Their synthesis can be done either by the ring-opening
43 polymerization of cyclic esters, or by polycondensation reactions. The conventional method for the
44 polycondensation of aliphatic monomers uses metal-based catalysts and requires elevated

45 temperatures [5–7]. However, reactions using metal-based catalysts can suffer from certain issues
46 such as color changes, degradation due to high temperature, lack of selectivity and difficulty in the
47 removal of residual metals from the synthesized polymer [8,9]. Accordingly, these recent years have
48 witnessed a growing research on replacing metal-based catalysts with more eco-friendly
49 organocatalysts and enzymes, both of which possessed certain advantages and limitations.[10] This
50 work will focus on enzymatic catalysis as a replacement to conventional metal-based catalysts, due
51 to their selectivity, eco-friendly, and recyclable nature [5,10–16]. The most popular biocatalyst used
52 is Novozym 435 (N435 - lipase B from *Candida Antarctica* immobilized on an acrylic resin), where
53 it showed improved properties in terms of specificity, thermal stability, and selectivity, and was
54 proposed in many research works as a versatile catalyst that can be beneficial in different synthetic
55 routes, particularly in the case of aliphatic polyesters [17,18]. For instance, the large scale production
56 of aliphatic polyesters via enzymatic catalysis was reported using adipic acid and 1,6-hexanediol as
57 monomers and N435 as a catalyst [19]. Another polyester, poly(butylene succinate) was synthesized
58 via enzymatic polycondensation of diethyl succinate and 1,4-butanediol both in organic solvent and
59 in bulk conditions [20]. N435 was reported as a catalyst for the combination of ring-opening
60 polymerization and polycondensation reactions using glycidol, ω -pentadecalactone, and adipic acid
61 as starting materials [21]. Similarly, ω -pentadecalactone, diethyl succinate and 1,4-butanediol were
62 catalyzed via CALB yielding a 77,000 g.mol⁻¹ polyester [10,22]. Regarding its regioselectivity,
63 Kulshrestha et al. [23] reported the biosynthesis (N435) of linear copolyesters starting with glycerol,
64 1,8-octanediol, and adipic acid. The regioselectivity towards primary alcohol esterification was
65 between 77 to 82%. Similarly, Zeng et al. showed that in the polycondensation of glycerol, 1,8-
66 octanediol and adipic acid, N435 produced a close to linear polyester, where the selectivity of
67 acylation at the primary hydroxyl sites of glycerol was 74.9 %, and the number average molecular
68 weight (M_n) achieved was 22,700 g.mol⁻¹. Those results were superior to other catalysts such as
69 scandium triflate and organocatalysts such as 1,5,7-triazabicyclo[4,4,0]dec-5-ene (TBD), diphenyl
70 hydrogen phosphate, and bis(1,1,2,2,3,3,4,4,4-nonafluoro-1-butanefluoronyl)imide, that did not
71 exceed a selectivity 65.9 % or yield molecular weights higher than 6,000 g.mol⁻¹ [24].

72 Many of the research in the area of enzymatic polyesterification remains very empirical, *i.e.*
73 testing the viability and efficiency of different enzymes for the development of polyesters and
74 optimizing the reaction conditions for achieving high molecular weights. However, the impact of
75 certain parameters, or in a more accurate sense, the 'degree of impact' of these parameters can vary
76 largely in different conditions and settings. Passing from solution to bulk remains very challenging
77 and certain parameters, such as vacuum application can behave differently. Although the importance
78 of vacuum in the two-step method is very well established [5,25–27], most research included vacuum
79 at a constant value, or otherwise compared it to reactions under atmospheric pressure. Poojari *et al.*
80 [28] showed that an increase in vacuum gauge pressure from 66 to 400 mbar resulted in a significant
81 increase in M_n in the polycondensation reactions between 1,3-bis(3-
82 carboxypropyl)tetramethyldisiloxane and 1,4-butanediol or 1,6-hexanediol. In the presence of 1,8-
83 octanediol, the vacuum effect was reversed. Jiang [22] showed the necessity of high vacuum
84 application to synthesize high molecular weight copolymers of ω -pentadecalactone, diethyl
85 succinate, and 1,4-butanediol, by comparing the results achieved at high vacuum (<4 mbar) to very
86 low levels of vacuum being ~ 800 and 1,013 mbar (atmospheric pressure) respectively, where the two
87 latter conditions produced oligomers that did not exceed 1,000 g.mol⁻¹ in M_n compared to values
88 exceeding 10,000 g.mol⁻¹ at high vacuum levels.

89 Traditional methods of optimization follow a one-factor-at-a-time approach (OFAT), which
90 involves varying one factor while keeping other factors constant. The main drawback of this method
91 is that it does not account for interactions between the tested variables, leading to inaccuracy in
92 depicting the true effect of the factors tested. On the other hand, the use of response surface
93 methodology (RSM) such as central composite design (CCD) allows for an accurate representation of
94 the effect of the tested variables and their interaction [29]. RSM has been successfully employed in
95 many research works as a tool of optimization [30,31]. For example, Itabaiana *et al.* [32] used a CCD
96 to determine optimal conditions for lipase catalyzed esterification of waste fatty acids into useful

97 esters. Similarly, Pellis *et al.* [33] used a fractional factorial design to evaluate the effect of temperature,
98 pressure, and water content in the polycondensation reaction between 1,4-butanediol or 1,8-
99 octanediol with dimethyl adipate catalyzed by either cutinase 1 from *Thermobifida cellulosilytica* or
100 CALB, under solvent and thin film conditions.

101 In order to implement our response surface methodology, we select the step-growth synthesis
102 of poly(hexylene adipate) conducted in solution and in bulk, following a two-step procedure,
103 transesterification followed by polycondensation. After assessing the influence of oligomerization
104 time and monomer concentration, the variable impact and interaction of different experimental
105 parameters (temperature, % w/w enzyme loading, and vacuum) on the polycondensation reaction
106 between 1,6-hexanediol and diethyl adipate in solvent (diphenyl ether) and bulk media, using N435
107 is reported. Two central composite designs were used to build second order quadratic models with
108 equations that can predict the M_n based on the conditions used. As such, these models give users the
109 exact parameters that can be considered to develop a polymer with a certain desired range of M_n , a
110 method that can show to be very useful for providing an efficient tool in the enzymatic synthesis of
111 polyesters using a step-growth method, where the control of M_n is of importance. Finally, the
112 influence of the process, bulk *vs.* solution, on enzyme recycling was also studied.

113 2. Materials and Methods

114 2.1. Materials

115 1,6-hexanediol (97%), diethyl adipate (99%) and diphenyl ether (99%) were purchased from
116 Sigma-Aldrich. Analytical grade methanol, tetrahydrofuran (THF), chloroform (99%) and toluene
117 were purchased from VWR. All the reagents and solvents were used as received. Novozym 435
118 (N435), a *Candida antarctica* Lipase B (CALB) immobilized on an acrylic resin was kindly provided
119 by Novozymes (activity = 10,000 propyl laurate units (PLU)/g). Chloroform D (CDCl₃) (99.8%) was
120 purchased from Euriso-top.

121 2.2. General procedure of the enzymatic polycondensation of 1,6-hexanediol and diethyl adipate

122 Equimolar amounts (4 mmol) of 1,6-hexanediol and diethyl adipate were weighed and added
123 into a schlenk tube. A predetermined amount varied between 1 and 10% w/w of N435 (relative to the
124 total weight of the monomers) was weighed and added to the mixture. For solution polymerization,
125 1 mL of diphenyl ether was added as a solvent of choice, whereas for bulk polymerization, the
126 reaction was commenced with no additional steps. The reaction proceeded under atmospheric
127 pressure for 2 h at a preset temperature between 80 and 100 °C (using an oil bath with continuous
128 stirring kept constant at 350 rpm). Afterwards, the schlenk tube was attached to a vacuum line, and
129 the pressure was decreased gradually in 1 h to reach a predetermined value between 10 and 50 mbar
130 to remove byproduct (ethanol). After applying the vacuum, the reaction was left to proceed for 24 h
131 and got stopped by adding an excess amount of chloroform under atmospheric pressure after a
132 cooling step, followed by direct filtration to remove the N435 beads. The filtrate was then partially
133 evaporated using a rotavap, and then added dropwise to excess amount of cold methanol under
134 stirring to precipitate the obtained polymer. The mixture was then filtered, and the product obtained
135 was left to dry at room temperature for 24 h before collecting and weighing.

136 2.3. Effect of solvent volume on the achieved number-average molecular weight (M_n)

137 For solution polymerization, diphenyl ether was chosen as a solvent. To determine the effect of
138 volume variation, the polycondensation reaction was carried out with different volumes at 100 °C at
139 1% w/w N435 for 2 h oligomerization followed by an additional 24 h polymerization under 10 mbar
140 of vacuum (see Table 1). The reaction was then confirmed via ¹H NMR analysis.

141 2.4. Effect of the oligomerization step time on conversion in solution and bulk

142 The conversion was monitored by exploiting the ^1H NMR signals at $\delta = 4.11\text{--}4.14$ of the
143 methylene group ($\text{CH}_3\text{-CH}_2\text{-O-}$) of diethyl adipate (DEA) in addition to the signals at $\delta = 4.06$ of the
144 methylene ($\text{-O-CH}_2\text{-C}_4\text{H}_8\text{-CH}_2\text{-O-}$) of the poly(hexylene adipate). Conversion was calculated via the
145 ratio of the signal representing poly(hexylene adipate) at $\delta = 4.06$ relative to the summation of signals
146 representing DEA and poly(hexylene adipate) at $\delta = 4.11\text{--}4.13$ and at $\delta = 4.06$, respectively (see
147 Equation S1 in supporting information). Examples of NMR spectra are presented in Figure S4 and S5.

148 2.5. Effect of the oligomerization step time on the achieved number-average molecular weight (M_n) after 24 h 149 of post vacuum application in bulk

150 Two-step polycondensation reactions were set up to run with a tunable oligomerization time (2,
151 4, and 6 h) at constant temperature (90 °C), % w/w enzyme loading (5.5%), and followed by a
152 secondary 24 h step under vacuum (10 mbar) application. M_n was determined by GPC analysis.

153 2.6. N435 recyclability

154 The polycondensation protocol of 1,6-hexandiol and diethyl adipate was followed as mentioned
155 before, the temperature was kept constant at 100 °C and the oligomerization step at 2 h. At the end
156 of each polymerization cycle, the separated N435 beads were washed 3 times with excess chloroform,
157 then left to dry at room temperature for 24 h under atmospheric pressure and reused for three
158 consecutive cycles.

159 2.7. Analytical methods

160 2.7.1. ^1H NMR analysis

161 Approximately 5 mg of 1,6-hexanediol, diethyl adipate, and the recovered poly(hexylene
162 adipate) were directly dissolved in three NMR tubes containing 0.5 mL of CDCl_3 . The ^1H NMR spectra
163 of the monomers, and the recovered polymer were recorded at room temperature on a Bruker Avance
164 300 instrument (delay time = 3 s, number of scans = 32) at 300.13 MHz. Chemical shifts (ppm) are
165 given in τ -units and were calibrated using the residual signal of CDCl_3 at 7.26 ppm. Additionally, ^1H
166 NMR was used to confirm conversion (detailed in supporting information). Data acquisition and
167 analysis were performed using the Bruker TopSpin 3.2.

168 2.7.2. GPC analysis

169 Gel permeation chromatography analysis was performed in THF as eluent (flow rate of 1
170 mL/min) at 40 °C using Alliance e2695 (Waters) apparatus and with a sample concentration around
171 10–15 mg/mL. A refractive index detector Optilab T-rEX (Wyatt Technology) was used as a detector,
172 and a set of columns: HR1, HR2 and HR4 (Water Styragel) were utilized. The molecular weight
173 calibration curve was obtained using monodisperse polystyrene standards.

174 2.7.3. MALDI-MS analysis

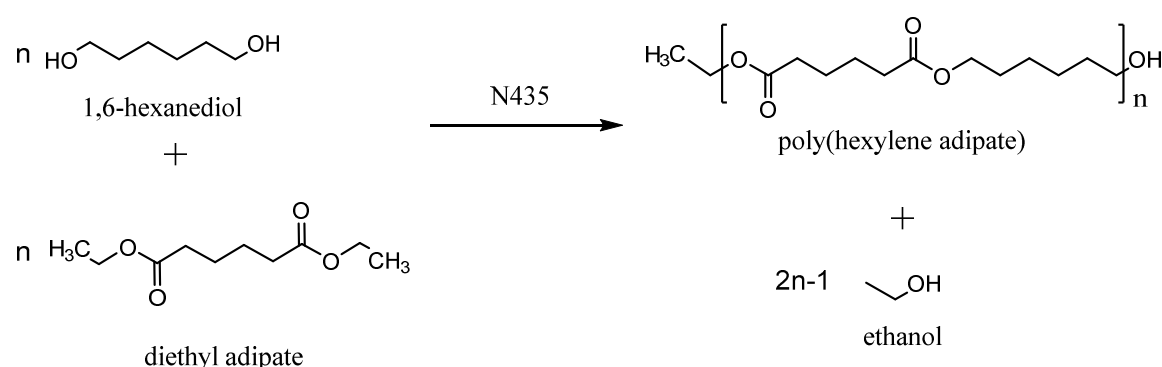
175 Positive-ion Matrix assisted LASER Desorption/Ionization-Mass Spectrometry (MALDI-MS)
176 experiments were performed using a Waters QToF Premier mass spectrometer equipped with a
177 Nd:YAG laser operating at 355 nm (third harmonic) with a maximum output of 65 μJ delivered to
178 the sample in 2.2 ns pulses at 50Hz repeating rate. Time-of-flight mass analysis was performed in the
179 reflectron mode at a resolution of about 10 k (m/z 569). All samples were analyzed using trans-2-[3-
180 (4-tert-butylphenyl)-2-methylprop-2-enylidene]malononitrile (DCTB) as a matrix. Polymer samples
181 synthesized in bulk as well as in solution conditions were dissolved in THF to obtain 1 $\text{mg}\cdot\text{mL}^{-1}$
182 solution. Additionally, 40 μL of 2 $\text{mg}\cdot\text{mL}^{-1}$ NaI solution in acetonitrile was added to the polymer
183 solution.

184 2.8. Statistical analysis

185 A face centered central composite design (CCD) was used to optimize the polycondensation
 186 reaction of poly(hexylene adipate) in terms of the established number-average molecular weight
 187 (M_n). A CCD is an experimental designed used to determine the effect and interaction of several
 188 factors and develop a response model. This design consists of 3 levels represented as (-1, 0, 1), where
 189 the center point (0) is replicated several times to determine variability and improve predictability. In
 190 the following work, 3 factors were tested at 3 levels being temperature (80, 90, 100 °C), % w/w enzyme
 191 loading (1, 5.5, 10%), vacuum (10, 30, 50 mbar). The models were developed and analyzed by Design-
 192 Expert 11®. The models were confirmed by running additional experiments that fell within 95% PI
 193 (prediction interval) range (see Table S 4 and Table S 8).

194 3. Results

195 The solution polycondensation of equimolar amounts (4 mmol) of 1,6-hexanediol and diethyl
 196 adipate in the presence of N435 (see Scheme 1) was conducted in diphenyl ether, as it was reported
 197 to be the more suitable solvent to achieve higher molecular weights [20,34].



Scheme 1. Polycondensation of 1,6-hexanediol and diethyl adipate in the presence of N435 as catalyst.

198 **Table 1.** Effect of monomer concentration on yield, M_n and dispersity of poly(hexylene adipate).

Entry ¹	Concentration (mol.L ⁻¹)	Yield (%)	M_n (g.mol ⁻¹) ²	\bar{M}_w ³
1	4	88	12,300	1.44
2	2	86	10,700	1.49
3	1	74	8,300	1.30
4	0.5	56	7,400	1.18

199 ¹ All experiments were conducted following a two-step polycondensation reaction: 1st step reaction
 200 conducted under atmospheric pressure, followed by the 2nd step of 24 h under vacuum (10 mbar).
 201 Temperature and enzyme loading were kept constant in both steps at 100 °C and 10% w/w of N435. ²
 202 The number average molecular weight (M_n) was obtained from GPC analyses (CHCl₃, 40 °C,
 203 polystyrene standards). ³ Molar mass dispersity $\bar{M}_w = M_w/M_n$ was obtained from GPC analyses
 204 (CHCl₃, 40 °C, polystyrene standards).

205 The effect of the concentration on the yield and molecular weight was first assessed considering
 206 a 2 h oligomerization step followed by a 24 h polycondensation step under a vacuum of 10 mbar and
 207 a temperature of 100 °C. The overall concentrations were varied by changing the amount of diphenyl
 208 ether used. A typical ¹H NMR spectrum is provided in the SI section (Figure S3), and the results are
 209 given in Table 1. **Erreur ! Source du renvoi introuvable.** An increase in M_n and yield with monomer
 210 concentration can be noticed, e.g. where the M_n passed from 7,400 up to 12,300 g.mol⁻¹ by increasing
 211 the monomer concentration from 0.5 to 4 mol.L⁻¹. Similarly, the yield increased from 56 to 88%.
 212 Therefore, for the next experiments carried out in solution, the volume of diphenyl ether was set
 213 constant at 1 mL to establish a monomer concentration of 4 mol.L⁻¹. This decrease in M_n as a function

214 of decreasing monomer concentration can be attributed to the decrease in the polymerization rate in
 215 dilute solutions due to the decrease in molecular collision as proposed by the collision theory [22,23].
 216 In fact, this drop in reactivity is reflected as a decrease in monomer conversion which would decrease
 217 the degree of polymerization (X_n) according to Carothers equation: $X_n = 1/(1 - p)$ where p is
 218 defined as the conversion [35]. Another proposed cause can also be attributed to the decrease in the
 219 byproduct (ethanol) removal efficiency in lower concentration solutions [36]. As the vacuum
 220 application may result in the evaporation of small monomer fractions, the oligomerization step was
 221 varied between 1 and 6 h in both bulk and solution in order to determine a suitable time for oligomer
 222 growth before the vacuum application. 1,6-hexanediol and DEA were added in equimolar amounts
 223 (4 mmol) in both systems, while 1 mL of diphenyl ether was added for the solution polymerization
 224 method to obtain the previously optimized concentration (4 mol.L⁻¹) conditions. The monomer
 225 conversion after the first step was determined via ¹H NMR (see Figure S4, S5) at different time
 226 intervals in order to assess the reaction kinetics and the time needed to reach the equilibrium at
 227 different temperatures and % enzyme loading, as reported in Figure 1.

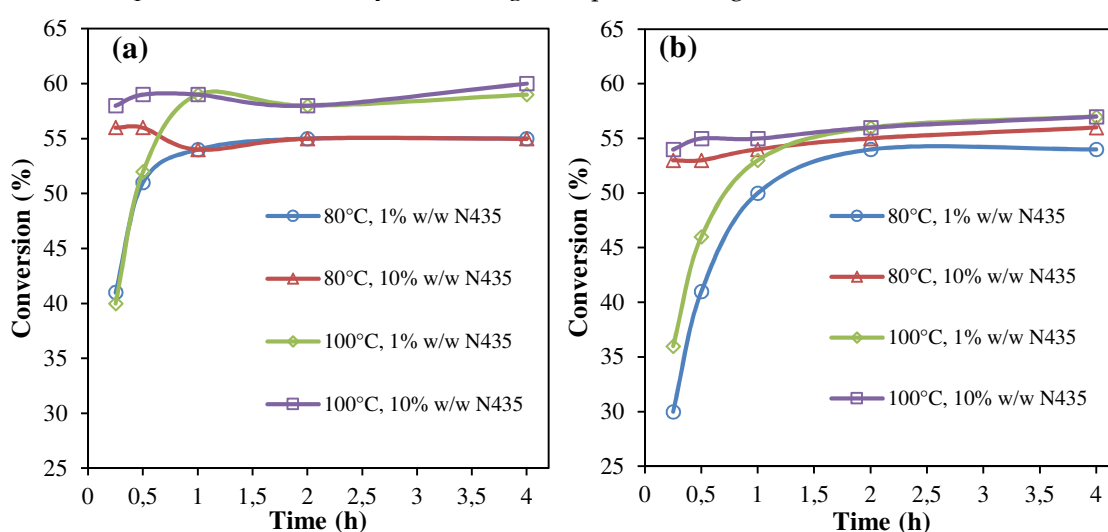


Figure 1. Conversion (expressed in %) after oligomerization step calculated via ¹H NMR as a function of temperature and enzyme loading in bulk (a) and diphenyl ether (b) conditions.

228 From Figure 1, it was noticed that the increase in % enzyme loading from 1 to 10% affected the
 229 rate of conversion, while at 10% enzyme, the maximum conversion reached a maximum within a
 230 time of 15 min in both solution and bulk, compared to 1 and 2 h with 1% N435 in both bulk and
 231 diphenyl ether conditions respectively. On the other hand, a temperature increase of 20 °C did not
 232 influence the reaction rate, but rather increased the maximum monomer conversion by a modest
 233 value of ~4%.

234 To validate the 2 h oligomerization step, a two-step polycondensation reaction was set up to run
 235 at constant temperature, % enzyme loading, and vacuum. This test was set to determine if extending
 236 the oligomerization time would have any effect on the M_n of the final product after a 24 h vacuum
 237 application. The corresponding conditions are enclosed in Table 2 where the only variable was the
 238 oligomerization time, followed by a 24 h of vacuum application. The results confirm that, for an
 239 average value of 5.5 w/w of enzyme, there is no influence between 2 or 6 h oligomerization time
 240 where, e.g., the M_n after 24 h were 6,700, 7,000, and 6,700 g.mol⁻¹ for 2, 4, and 6 h oligomerization
 241 respectively. In other words, there is no need for prolongation, and an oligomerization step of 1 or 2
 242 h is sufficient for further experiments.

243 **Table 2.** Effect of oligomerization time variation on yield, M_n , and dispersity after a 24 h (secondary
 244 step) under vacuum.

Entry	Reaction time (h) ¹ 1 st step/ 2 nd step	Yield (%)	M_n (g.mol ⁻¹) ²	\overline{M}_w ³
-------	--	-----------	---	-------------------------------

5	2/ 24	88	6,700	1.38
6	4/ 24	86	7,000	1.34
7	6/ 24	74	6,700	1.38

245 ¹ 1st step reaction conducted under atmospheric pressure, followed by the 2nd step of 24 h under
 246 vacuum (30 mbar). Temperature and enzyme loading were kept constant in both steps at 90 °C and
 247 5.5% w/w of N435. ² The number average molecular weight (M_n) was obtained from GPC analyses
 248 (CHCl₃, 40 °C, polystyrene standards). ³ Molar mass dispersity $D_M = M_w/M_n$ was obtained from GPC
 249 analyses (CHCl₃, 40 °C, polystyrene standards).

250 Although the effect of temperature and catalyst loading were widely studied in the literature,
 251 the effect of vacuum variation was scarcely mentioned. The results obtained using the central
 252 composite design (CCD) of experiment did not only determine the effect of temperature, % enzyme
 253 loading, and vacuum, but also the interactions between these factors. For solution polymerization,
 254 and following the method detailed under statistical analysis (Experimental section), a quadratic
 255 model was developed with a predicted $R^2=0.92$, the predicted vs. actual results and other statistical
 256 results are given in the supporting information section and show a very good fit of the data. The
 257 model is presented as an equation in terms of the actual factors given in Table S3.

258 After a 24 h reaction under vacuum, ¹H NMR confirmed >90% conversion for all samples (sample
 259 results are provided in the supporting sheet Figure. S6 & S7).

260 As for the effect of the tested variables, the results clearly show that vacuum was the most
 261 influential factor on the M_n achieved, where an increase from 50 to 10 mbar resulted in an increase of
 262 4,400 g.mol⁻¹ at 80 °C and up to 6,300 g.mol⁻¹ at 100 °C showing that vacuum becomes more influential
 263 at elevated temperatures. Similarly, the temperature increase had a pronounced effect on the M_n ,
 264 where an increase of 20 °C from 80 to 100 °C resulted in an increase in M_n by 3,300 g.mol⁻¹ when the
 265 vacuum was 10 mbar. The effect of temperature did not have the same influence at the lower vacuum
 266 level of 50 mbar where the same temperature increase, resulted only in 1,400 g.mol⁻¹ increase in M_n
 267 (see Figure 2 (a)) increased with the increase in M_n , with all values within a range of 1.2-1.7 (see Table
 268 S9). These results arise from a significant interaction between variables, which in this case is an
 269 interaction between temperature and vacuum. In other words, the effect of vacuum on M_n is
 270 dependent on the level of temperature and *vice versa*. This vacuum-temperature interaction could be
 271 further justified by Clausius-Clapeyron equation where the vapor pressure of liquids increases with
 272 the increase in temperature in a non-linear manner [37,38], and thus, at higher temperatures, vacuum
 273 application becomes more efficient in the removal of ethanol due to a more pronounced increase in
 274 vapor pressure, thus pushing the reaction forward. Additionally, varying the % enzyme loading
 275 between 1 and 10% showed no significant effect on M_n (see Figure 2(b), Figure 2(c), suggesting that
 276 with 1% w/w N435, the catalyst exceeds the stoichiometric amount of reactive moieties present in the
 277 system and is therefore sufficient to catalyze the reaction.

278 Moving into bulk polymerization, a quadratic model was designed with an $R^2=0.9$ using the
 279 same variables and levels as in solution polycondensation conditions to facilitate comparison. The
 280 equation is given in Table S7 and further statistical information is provided in the supporting
 281 information. However, in contrary to the results in solution, the factors tested here had different
 282 influence on the M_n of the synthesized polymer, where it was shown that enzyme loading had the
 283 most pronounced effect (see Figure 2(d), Figure 2(e)), followed by temperature, and finally vacuum
 284 (see Figure 2(f)) giving a less pronounced effect. Additionally, the M_n achieved in bulk conditions
 285 was significantly lower than that achieved in solution following the same conditions. Dispersity (see
 286 Table S9) increased with M_n but did not vary beyond the range of 1.2-1.6. These variations are not
 287 surprising. In fact, it could be explained by the decrease in diffusion capabilities of growing chains in
 288 high viscous mediums. In contrast to solution polymerization, bulk polymerization shows fast and
 289 significant increase in viscosity within minutes of vacuum application, leading to complete stop of
 290 stirring applied via magnetic bars. Having the catalyst in its heterogeneous form, it becomes more
 291 and more crucial to maintain adequate mass transfer to allow the polymer growth. In fact, though
 292 1% N435 proved to be as efficient as 10% in solution, the results in bulk conditions showed significant
 293 variation between both percentages. This variation should be mainly attributed to the limitations

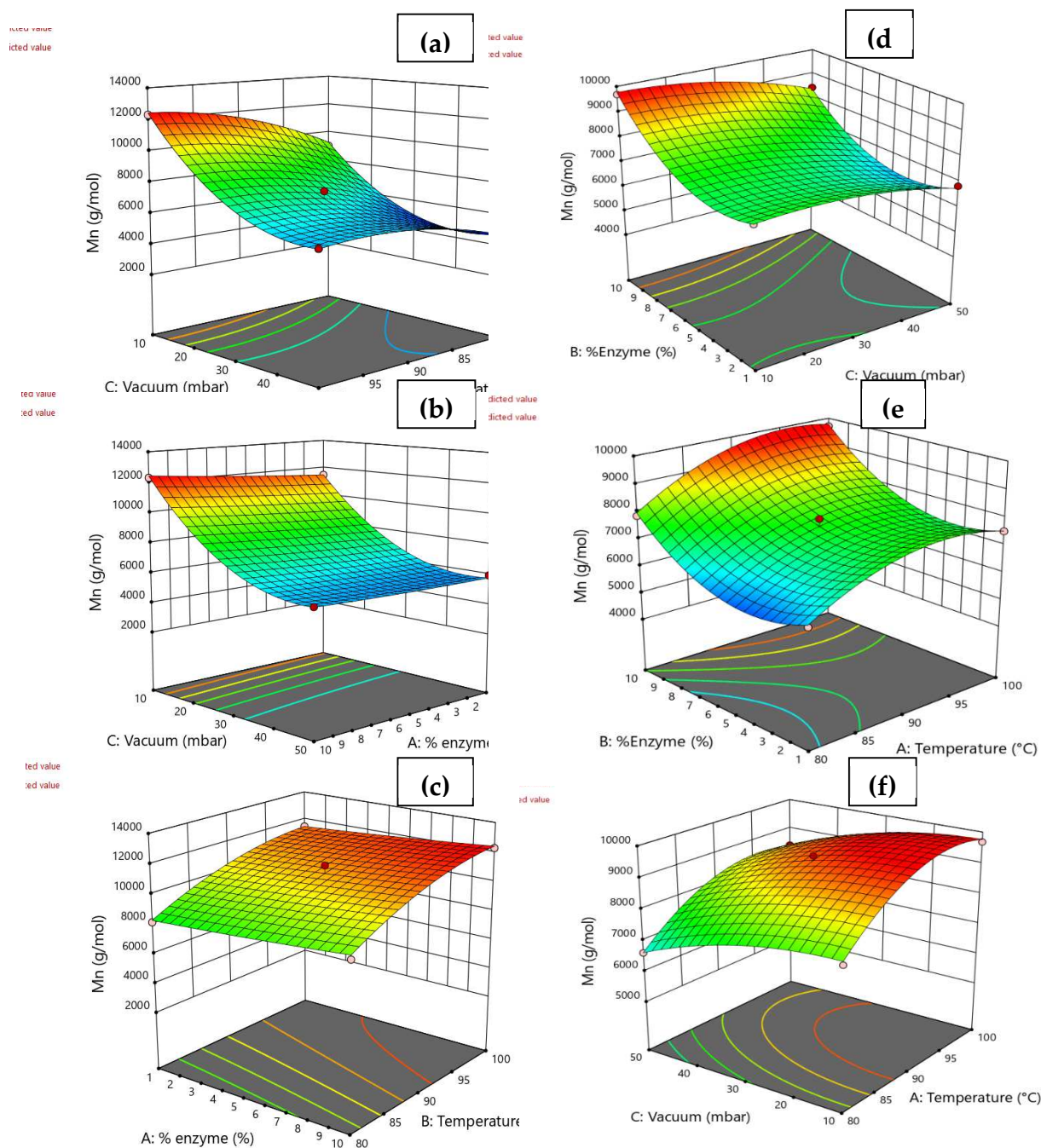


Figure 2. (a) Effect of vacuum and temperature on M_n (solution) at 10% enzyme loading. (b) Effect of vacuum and % enzyme loading on M_n (solution) at 100 °C. (c) Effect of % enzyme loading and temperature on M_n (solution) at 10 mbar of reduced pressure. (d) Effect of vacuum and % loading enzyme on M_n (bulk conditions) at 100 °C. (e) Effect of % enzyme loading and temperature on M_n (bulk conditions) at 10 mbar of vacuum. (f) Effect of vacuum and temperature on M_n (bulk conditions) at 10% enzyme loading. *(The red and pink points represent experimental data above and below the predicted model respectively).

294 enforced by the decrease in mass transfer rather than the activity of the enzyme, where a higher
 295 loading of N435 would rationally occupy more space within the medium, resulting in more
 296 interaction between substrates and the enzyme active sites especially when chain movement in the
 297 medium is reduced. Blank reactions (without enzyme) were performed in both solution and bulk
 298 conditions at 100 °C for (2 h oligomerization under atmospheric pressure, followed by 24 h under 10
 299 mbar of vacuum. However, no precipitates were formed with cold methanol, suggesting that no
 300 polymer growth was achieved without N435.

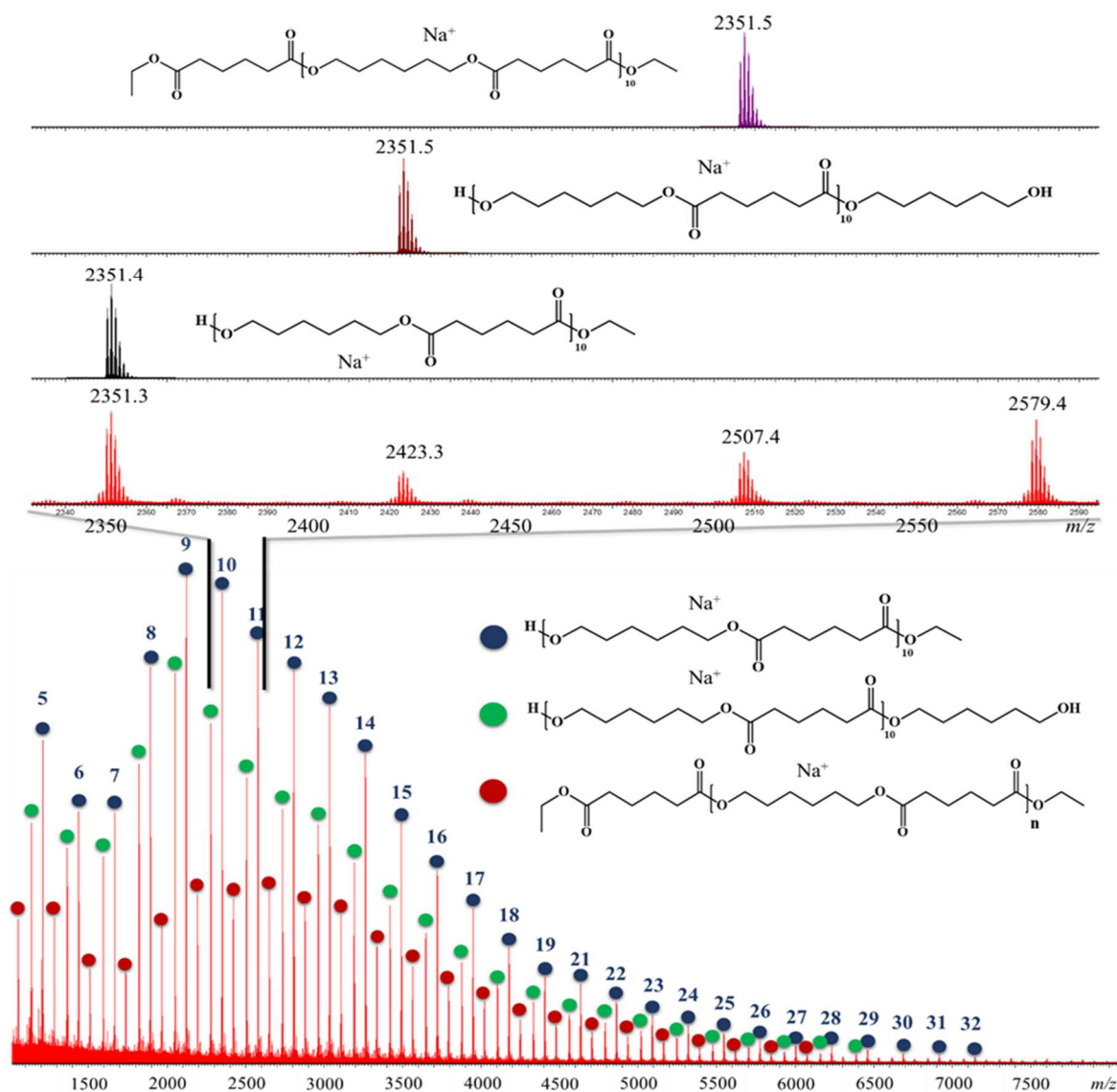


Figure 3. MALDI mass spectrum recorded for experiment 1S, lower part of the figure represents the global mass spectrum with the 3 main families present in the polymer sample, the number on each signal highlights the number of monomer units for the observed ions. The upper part of the spectrum corresponds to a magnification between m/z 2300 and m/z 2600 with a comparison between the theoretical isotopic models (for oligomers with 10 monomer units of diol and diester) and the experimental data confirming the presence of 3 end-groups moieties i.e. ester-ester (red dots), alcohol-alcohol (green dots) and ester-alcohol (blue dots) respectively.

301 MALDI-ToF MS was used to determine the nature of the end-groups present in the synthesized
 302 poly(hexylene adipate). However, due to the quite broad molar mass dispersity (i.e. >1.2) of the
 303 polymer samples, mass spectrometry was not useful for determining the molar masses accurately
 304 [39]. As such, 16 polymer samples (8 solution and 8 bulk conditions) were analyzed to establish a
 305 comparison between both conditions as represented in Table S9. From the MS spectra in

306 Figure 3 representing experiment 1S, three main polyester families were identified being end-
 307 functionalized as (1) ester-ester (2) alcohol-alcohol (3) ester-alcohol. Cyclic structure was also
 308 probable but only traces were detected. Based on the MALDI spectrum, ester-alcohol was found to
 309 possess the highest intensity, showing that these structures are the most abundant in the sample, as
 310 expected. Those results were consistent among all the tested samples in bulk and solution media with
 311 no apparent differences.

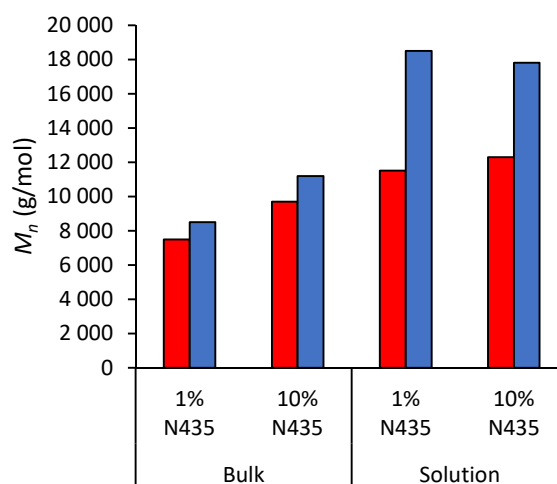


Figure 4. Effect of extending polymerization time on M_n in both solution and bulk conditions.

312 The limitation imposed by the decrease in mass transfer becomes more apparent when
 313 extending the reaction time (see Figure 4), where the M_n of polyesters synthesized in bulk increase
 314 only by 30% when extending the reaction time from 24 to 48 h. On the other hand, up to 70% increase
 315 in M_n was observed in solution, mainly due to both better mixing and mass transfer. The high positive
 316 influence of efficient mixing was previously highlighted using reactive extrusion for the ring-opening
 317 polymerization of ω -pentadecalactone, yielding an M_n of 90,000 g.mol⁻¹ in only 15 min compared to
 318 22,100 g.mol⁻¹ after 72 h in bulk conditions [40]. In this work, the M_n of the first cycle in both mediums
 319 was considered as 100%, while the percentage yield was calculated by dividing the actual yield by
 320 the theoretical yield, taking into consideration the molar mass of the polyester achieved.

321 The recyclability of N435 was finally tested for three consecutive cycles in solution (1% w/w
 322 N435) (see Figure 5) and bulk conditions (0.5, 1, and 10% w/w N435) (see Figure 6). The results for
 323 solution polycondensation showed ~17% drop in M_n during the second cycle from 12,100 to 10,000
 324 g.mol⁻¹, however, no significant changes were observed during the third cycle.

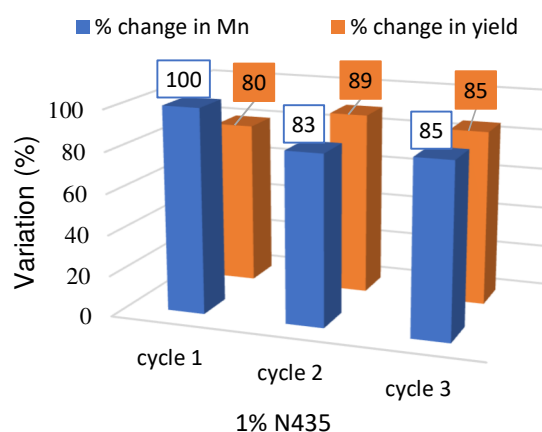


Figure 5. Effect of recycling 1% N435 on M_n and yield in solution.

325 On the other hand, the recyclability assays in bulk conditions showed better consistency during
 326 the three cycles where the M_n dropped by a maximum of 8% in the third cycle with 1% N435, and to
 327 a lower extent with 0.5 and 10% N435, knowing that it was considered insignificant as it falls within
 328 the error range of the GPC analysis. As such, for bulk polymerization, even at relatively high
 329 temperature (100 °C), N435 can be effectively reused at least for three consecutive cycles giving
 330 similar results in terms of M_n and yield as observed in Figure 6. The more pronounced drop in N435
 331 activity in diphenyl ether medium can be attributed to several reasons. First, the use of diphenyl ether
 332 as a solvent attributed to a better heat transfer in the system, and thus, the enzyme will be more prone
 333 to elevated temperatures in comparison to bulk, which would result in a more pronounced enzyme
 334 degradation or leaching. Additionally, due to the fact that N435 is prepared via interfacial activation
 335 of lipases *vs.* supports with hydrophobic surfaces, the enzyme becomes more susceptible to be
 336 released in the presence of organic solvents [17,41,42]. Moreover, the activity of enzymes can also be

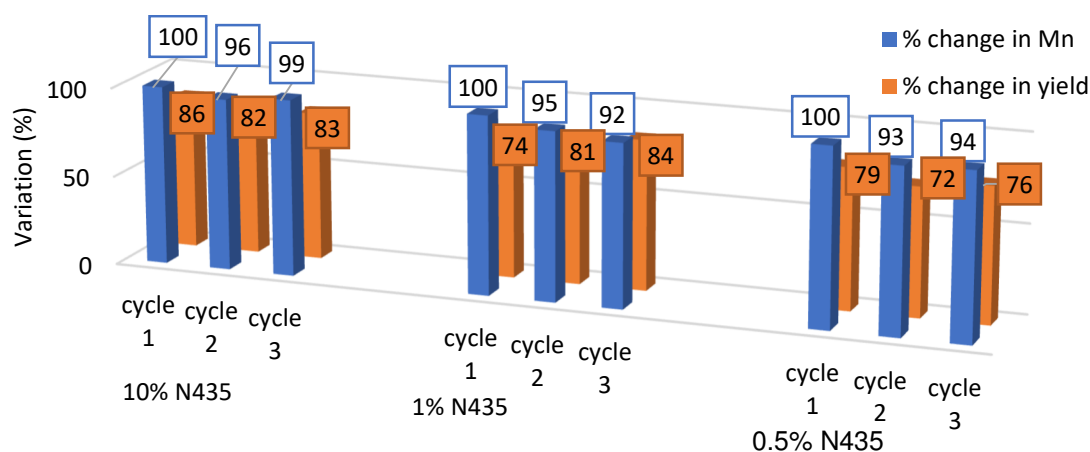


Figure 6. Effect of recycling 0.5, 1 and 10% N435 on M_n and yield in bulk conditions.

337 influenced by the water activity, Secundo et al. showed a drop in the transesterification activity for
 338 the reaction between vinylacetate and 1-octanol as a function of water activity in different
 339 formulations of CALB, including N435 [43]. Similarly, other works found a similar relation between
 340 the increase in water activity and the decrease in enzyme activity and maximum achieved M_n [44–
 341 47].

342 However, this remains a speculation within the current study and further studies are needed to
 343 determine the reason behind the drop in N435 activity in solution.

344 4. Conclusions

345 The polycondensation reaction of 1,6-hexanediol and diethyl adipate was studied in both
 346 diphenyl ether and bulk media using Novozym 435 as biocatalyst. The oligomerization time was
 347 optimized where the maximum monomer conversion was confirmed after a maximum of 2 h from
 348 the start of the reaction, thus preventing any unnecessary time extension for the oligomerization step.
 349 Following, a face centered central composite design was used to develop a quadratic model that
 350 showed how temperature, vacuum, and % enzyme loading can affect M_n . In diphenyl ether, vacuum
 351 showed to be the most influential factor in relation to M_n , followed by temperature, and finally %
 352 enzyme loading that showed no significant effect. This relation between the independent variables
 353 and M_n showed an opposite relation in bulk where % enzyme loading had the most significant impact
 354 on M_n , followed by temperature and vacuum respectively. The models were confirmed by running
 355 additional experiments, where their results were within the acceptable prediction interval,
 356 confirming that the models can be adequately used to predict the M_n of the polymer at any level
 357 within the tested factor ranges. Recyclability assays showed a more efficient recycling for N435 in
 358 bulk conditions (consistent results up to 3 cycles) in comparison to diphenyl ether that showed a drop
 359 of activity by 17% for the second cycle. Finally, this work introduced a green method to produce

360 poly(hexylene adipate) and control its M_n . Future research will enlarge on the findings of this work,
361 to develop efficient processes that would overcome some of the major limitations encountered herein,
362 such as low heat and mass transfer that limit polymer growth. Enzymatic reactive extrusion is
363 currently under investigation by our team as a powerful tool employed to surpass the
364 aforementioned obstacles and transform traditional batch production processes into more dynamic
365 continuous processes that can achieve high molecular weights within short periods of time.

366 **Supplementary Materials:** The following are available online at www.mdpi.com/xxx/s1, Figure S7: 1,6-
367 hexanediol ($C_6H_{14}O_2$) 1H NMR spectrum ($CDCl_3$, 300 MHz): δ 1.39 (m, 4H), 1.58 (m, 4H), 3.64 (t, $J = 6.5$ Hz, 4H);
368 Figure S8: Diethyl adipate ($C_{10}H_{18}O_4$) 1H NMR spectrum ($CDCl_3$, 300 MHz): δ 1.25 (t, $J = 7.1$ Hz, 6H), 1.66 (m,
369 4H), 2.31 (t, $J = 7.2$ Hz, 4H), 4.11-4.13 (q, $J = 7.1$ Hz, 4H); Figure S9: Poly(hexylene adipate) $[-O(CH_2)_6O_2C(CH_2)_4CO-$
370 $]_n$ 1H NMR spectrum ($CDCl_3$, 300 MHz): δ 1.37 (m, 4H), 1.66 (m, 8H), 2.32 (t, $J = 7.1$ Hz, 4H), 4.06 (t, $J = 6.7$ Hz,
371 4H); Figure S10: 1H NMR spectrum ($CDCl_3$, 300 MHz) of the crude reaction of 1,6-hexanediol and diethyl adipate
372 in diphenyl ether (1 mL), and the yielded Poly(hexylene adipate) after 15 mins reaction at 80 °C and 1% w/w
373 enzyme loading: δ 1.25 (t, 6H), 1.37 (m, 8H), 1.66 (m, 12H), 2.32 (t, 8H), 3.65 (t, 4H), 4.06 (t, 4H), 4.11-4.13 (q, 4H).
374 Note: $\delta \sim 7-7.5$ represent diphenyl ether; Figure S11: Enlarged view of figure S4: (between 2.2 and 4.2 ppm); Figure
375 S12: 1H NMR spectrum ($CDCl_3$, 300 MHz) of the crude reaction of 1,6-hexanediol and diethyl adipate in bulk,
376 and the yielded Poly(hexylene adipate) after 24 h at 50 mbar vacuum application, at 90 °C and 5.5% w/w enzyme
377 loading; Figure S13: 1H NMR spectrum ($CDCl_3$, 300 MHz) of the crude reaction of 1,6-hexanediol and diethyl
378 adipate in 1 mL diphenyl ether, and the yielded Poly(hexylene adipate) after 24 h at 10 mbar vacuum application,
379 at 100 °C and 1% w/w enzyme loading. Note: $\delta \sim 7-7.5$ represent diphenyl ether; Figure S14: Graph of the predicted
380 vs. actual plots in solution polymerization; Figure S15: Graph of the predicted vs. actual plots in bulk
381 polymerization; Table S1: Build information of the design model for in solution polymerization; Table S2: Fit
382 statistics for in solution polymerization; Table S3: Final equation in term of actual factors (in-solution
383 polymerization); Table S4: Additional tested point for model confirmation for in solution polymerization; Table
384 S5: Build information of the design model for bulk polymerization; Table S6: Fit statistics for bulk
385 polymerization; Table S7: Final equation in term of actual factors (bulk polymerization); Table S8: Additional
386 tested point for model confirmation for in solution polymerization; Table S9: Experiments analyzed via MALDI-
387 TOF MS for end group determination.

388 **Author Contributions:** Conceptualization, K.N., J.M., A.H.F., J.M.R., P.Z.; methodology, K.N.; software, K.N.;
389 formal analysis, K.N.; MALDI-TOF analysis, J.D.; writing—original draft preparation, K.N.; writing—review
390 and editing, K.N., J.M., A.H.F., J.D., J.M.R., and P.Z.; supervision, A.H.F., J.M.R., and P.Z.; project administration,
391 J.M.R. and P.Z.; funding acquisition, J.M.R. All authors have read and agreed to the published version of the
392 manuscript.

393 **Funding:** This work was funded by the FWV ALPO Interreg Grant and the authors thank the European Regional
394 Development Fund (FEDER) and the University of Lille. Chevreul Institute (FR 2638), Ministère de
395 l'Enseignement Supérieur, de la Recherche et de l'Innovation, Région Hauts de France are also acknowledged
396 for supporting and funding partially this work.

397 **Acknowledgments:** The authors are gratefully acknowledged to Aurélie Malfait and Jonathan Potier for GPC
398 measurements. The UMONS MS laboratory acknowledges the Fonds National de la Recherche Scientifique
399 (F.R.S.-F.N.R.S.) for its contribution to the acquisition of the Waters QToF Premier mass spectrometer and for
400 continuing support. JMR is a FNRS research fellow at University of Mons.

401 **Conflicts of interest:** There are no conflicts to declare.

402 References

- 403 1. Babu, R.P.; O'Connor, K.; Seeram, R. Current progress on bio-based polymers and their future trends.
404 *Prog Biomater* **2013**, *2*, 8, doi:10.1186/2194-0517-2-8.
- 405 2. Aeschelmann, F.; Carus, M. Biobased Building Blocks and Polymers in the World: Capacities,
406 Production, and Applications—Status Quo and Trends Towards 2020. *Industrial Biotechnology* **2015**, *11*,
407 154–159, doi:10.1089/ind.2015.28999.fae.
- 408 3. Hottle, T.A.; Bilec, M.M.; Landis, A.E. Sustainability assessments of bio-based polymers. *Polymer*
409 *Degradation and Stability* **2013**, *98*, 1898–1907, doi:10.1016/j.polymdegradstab.2013.06.016.

- 410 4. Hamaide, T.; Deterre, R.; Feller, J.-F. *Environmental Impact of Polymers*; John Wiley & Sons, 2014; ISBN
411 978-1-118-82709-3.
- 412 5. Douka, A.; Vouyiouka, S.; Papaspyridi, L.-M.; Papaspyrides, C.D. A review on enzymatic
413 polymerization to produce polycondensation polymers: The case of aliphatic polyesters, polyamides and
414 polyesteramides. *Progress in Polymer Science* **2018**, *79*, 1–25, doi:10.1016/j.progpolymsci.2017.10.001.
- 415 6. Fodor, C.; Golkaram, M.; Woortman, A.J.J.; Dijken, J. van; Loos, K. Enzymatic approach for the synthesis
416 of biobased aromatic–aliphatic oligo-/polyesters. *Polym. Chem.* **2017**, *8*, 6795–6805,
417 doi:10.1039/C7PY01559C.
- 418 7. Zong, Z.; Xu, J.; Xue, W.; Zeng, Z. Kinetics of the Esterification Reaction of Adipic Acid with 1,6-
419 Hexanediol Catalyzed by Tetraethyl Titanate. *Asian Journal of Chemical Sciences* **2018**, 1–11,
420 doi:10.9734/AJOCS/2018/46013.
- 421 8. Jacquel, N.; Freyermouth, F.; Fenouillot, F.; Rousseau, A.; Pascault, J.P.; Fuertes, P.; Saint-Loup, R.
422 Synthesis and properties of poly(butylene succinate): Efficiency of different transesterification catalysts.
423 *Journal of Polymer Science Part A: Polymer Chemistry* **2011**, *49*, 5301–5312, doi:10.1002/pola.25009.
- 424 9. Mochizuki, M.; Mukai, K.; Yamada, K.; Ichise, N.; Murase, S.; Iwaya, Y. Structural Effects upon
425 Enzymatic Hydrolysis of Poly(butylene succinate-co-ethylene succinate)s. *Macromolecules* **1997**, *30*, 7403–
426 7407, doi:10.1021/ma970036k.
- 427 10. Gross, R.A.; Ganesh, M.; Lu, W. Enzyme-catalysis breathes new life into polyester condensation
428 polymerizations. *Trends in Biotechnology* **2010**, *28*, 435–443, doi:10.1016/j.tibtech.2010.05.004.
- 429 11. Hilker, I.; Rabani, G.; Verzijl, G.K.M.; Palmans, A.R.A.; Heise, A. Chiral Polyesters by Dynamic Kinetic
430 Resolution Polymerization. *Angewandte Chemie International Edition* **2006**, *45*, 2130–2132,
431 doi:10.1002/anie.200503496.
- 432 12. Chaudhary, A.K.; Lopez, J.; Beckman, E.J.; Russell, A.J. Biocatalytic Solvent-Free Polymerization To
433 Produce High Molecular Weight Polyesters. *Biotechnology Progress* **1997**, *13*, 318–325,
434 doi:10.1021/bp970024i.
- 435 13. Kirk, O.; Christensen, M.W. Lipases from *Candida antarctica*: Unique Biocatalysts from a Unique Origin.
436 *Org. Process Res. Dev.* **2002**, *6*, 446–451, doi:10.1021/op0200165.
- 437 14. Kobayashi, S. Recent developments in lipase-catalyzed synthesis of polyesters. *Macromol Rapid Commun*
438 **2009**, *30*, 237–266, doi:10.1002/marc.200800690.
- 439 15. Lozano, P.; Diego, T. de; Carrié, D.; Vaultier, M.; Iborra, J.L. Lipase Catalysis in Ionic Liquids and
440 Supercritical Carbon Dioxide at 150 °C. *Biotechnology Progress* **2003**, *19*, 380–382, doi:10.1021/bp025759o.
- 441 16. Jiang, Y.; Woortman, A.J.J.; Ekenstein, G.O.R.A. van; Loos, K. A biocatalytic approach towards
442 sustainable furanic–aliphatic polyesters. *Polym. Chem.* **2015**, *6*, 5198–5211, doi:10.1039/C5PY00629E.
- 443 17. Ortiz, C.; Ferreira, M.L.; Barbosa, O.; Santos, J.C.S. dos; Rodrigues, R.C.; Berenguer-Murcia, Á.; Briand,
444 L.E.; Fernandez-Lafuente, R. Novozym 435: the “perfect” lipase immobilized biocatalyst? *Catal. Sci.*
445 *Technol.* **2019**, *9*, 2380–2420, doi:10.1039/C9CY00415G.
- 446 18. Hillmyer, M.A.; Tolman, W.B. Aliphatic Polyester Block Polymers: Renewable, Degradable, and
447 Sustainable. *Acc. Chem. Res.* **2014**, *47*, 2390–2396, doi:10.1021/ar500121d.
- 448 19. Binns, F.; Harffey, P.; Roberts, S.M.; Taylor, A. Studies leading to the large scale synthesis of polyesters
449 using enzymes. *J. Chem. Soc., Perkin Trans. 1* **1999**, 2671–2676, doi:10.1039/A904889H.
- 450 20. Azim, H.; Dekhterman, A.; Jiang, Z.; Gross, R.A. *Candida antarctica* lipase B-catalyzed synthesis of
451 poly(butylene succinate): shorter chain building blocks also work. *Biomacromolecules* **2006**, *7*, 3093–3097,
452 doi:10.1021/bm060574h.

- 453 21. Eriksson, M.; Fogelström, L.; Hult, K.; Malmström, E.; Johansson, M.; Trey, S.; Martinelle, M. Enzymatic
454 one-pot route to telechelic polypentadecalactone epoxide: synthesis, UV curing, and characterization.
455 *Biomacromolecules* **2009**, *10*, 3108–3113, doi:10.1021/bm9007925.
- 456 22. Jiang, Z. Lipase-catalyzed synthesis of aliphatic polyesters via copolymerization of lactone, dialkyl
457 diester, and diol. *Biomacromolecules* **2008**, *9*, 3246–3251, doi:10.1021/bm800814m.
- 458 23. Kulshrestha, A.S.; Gao, W.; Gross, R.A. Glycerol Copolyesters: Control of Branching and Molecular
459 Weight Using a Lipase Catalyst. *Macromolecules* **2005**, *38*, 3193–3204, doi:10.1021/ma0480190.
- 460 24. Zeng, F.; Yang, X.; Li, D.; Dai, L.; Zhang, X.; Lv, Y.; Wei, Z. Functionalized polyesters derived from
461 glycerol: Selective polycondensation methods toward glycerol-based polyesters by different catalysts.
462 *Journal of Applied Polymer Science* **2020**, *137*, 48574, doi:10.1002/app.48574.
- 463 25. Linko, Y.-Y.; Lämsä, M.; Wu, X.; Uosukainen, E.; Seppälä, J.; Linko, P. Biodegradable products by lipase
464 biocatalysis. *Journal of Biotechnology* **1998**, *66*, 41–50, doi:10.1016/S0168-1656(98)00155-2.
- 465 26. Linko, Y.-Y.; Wang, Z.-L.; Seppälä, J. Lipase-catalyzed synthesis of poly(1,4-butyl sebacate) from sebacic
466 acid or its derivatives with 1,4-butanediol. *Journal of Biotechnology* **1995**, *40*, 133–138, doi:10.1016/0168-
467 1656(95)00039-S.
- 468 27. Kosugi, Y.; Kunieda, T.; Azuma, N. Continual conversion of free fatty acid in rice bran oil to
469 triacylglycerol by immobilized lipase. *J Am Oil Chem Soc* **1994**, *71*, 445–448, doi:10.1007/BF02540528.
- 470 28. Poojari, Y.; Palsule, A.S.; Cai, M.; Clarson, S.J.; Gross, R.A. Synthesis of organosiloxane copolymers using
471 enzymatic polyesterification. *European Polymer Journal* **2008**, *44*, 4139–4145,
472 doi:10.1016/j.eurpolymj.2008.07.043.
- 473 29. Braiuca, P.; Ebert, C.; Basso, A.; Linda, P.; Gardossi, L. Computational methods to rationalize
474 experimental strategies in biocatalysis. *Trends in Biotechnology* **2006**, *24*, 419–425,
475 doi:10.1016/j.tibtech.2006.07.001.
- 476 30. Sarotti, A.M.; Spanevello, R.A.; Suárez, A.G. An efficient microwave-assisted green transformation of
477 cellulose into levoglucosenone. Advantages of the use of an experimental design approach. *Green Chem.*
478 **2007**, *9*, 1137–1140, doi:10.1039/B703690F.
- 479 31. Chang, S.-W.; Shaw, J.-F.; Yang, K.-H.; Shih, I.-L.; Hsieh, C.-H.; Shieh, C.-J. Optimal lipase-catalyzed
480 formation of hexyl laurate. *Green Chem.* **2005**, *7*, 547–551, doi:10.1039/B501724F.
- 481 32. Itabaiana, I.; Sutili, F.K.; Leite, S.G.F.; Gonçalves, K.M.; Cordeiro, Y.; Leal, I.C.R.; Miranda, L.S.M.; Ojeda,
482 M.; Luque, R.; Souza, R.O.M.A. de Continuous flow valorization of fatty acid waste using silica-
483 immobilized lipases. *Green Chem.* **2013**, *15*, 518–524, doi:10.1039/C2GC36674F.
- 484 33. Pellis, A.; Ferrario, V.; Cespugli, M.; Corici, L.; Guarneri, A.; Zartl, B.; Acero, E.H.; Ebert, C.; Guebitz,
485 G.M.; Gardossi, L. Fully renewable polyesters via polycondensation catalyzed by *Thermobifida*
486 *cellulosilytica* cutinase 1: an integrated approach. *Green Chem.* **2017**, *19*, 490–502,
487 doi:10.1039/C6GC02142E.
- 488 34. Mahapatro, A.; Kalra, B.; Kumar, A.; Gross, R.A. Lipase-catalyzed polycondensations: effect of substrates
489 and solvent on chain formation, dispersity, and end-group structure. *Biomacromolecules* **2003**, *4*, 544–551,
490 doi:10.1021/bm0257208.
- 491 35. Carothers, W.H. Polymers and polyfunctionality. *Trans. Faraday Soc.* **1936**, *32*, 39–49,
492 doi:10.1039/TF9363200039.
- 493 36. Jiang, Y.; Woortman, A.J.J.; Alberda van Ekenstein, G.O.R.; Loos, K. Enzyme-Catalyzed Synthesis of
494 Unsaturated Aliphatic Polyesters Based on Green Monomers from Renewable Resources. *Biomolecules*
495 **2013**, *3*, 461–480, doi:10.3390/biom3030461.

- 496 37. Speight, J.G. *Reaction Mechanisms in Environmental Engineering: Analysis and Prediction*; Butterworth-
497 Heinemann, 2018; ISBN 978-0-12-800667-2.
- 498 38. Speight, J.G. *Environmental Organic Chemistry for Engineers*; Butterworth-Heinemann, 2016; ISBN 978-0-
499 12-800668-9.
- 500 39. Martin, K.; Spickermann, J.; Räder, H.J.; Müllen, K. Why Does Matrix-assisted Laser
501 Desorption/Ionization Time-of-flight Mass Spectrometry Give Incorrect Results for Broad Polymer
502 Distributions? *Rapid Communications in Mass Spectrometry* **1996**, *10*, 1471–1474, doi:10.1002/(SICI)1097-
503 0231(199609)10:12<1471::AID-RCM693>3.0.CO;2-X.
- 504 40. Spinella, S.; Ganesh, M.; Re, G.L.; Zhang, S.; Raquez, J.-M.; Dubois, P.; Gross, R.A. Enzymatic reactive
505 extrusion: moving towards continuous enzyme-catalysed polyester polymerisation and processing.
506 *Green Chem.* **2015**, *17*, 4146–4150, doi:10.1039/C5GC00992H.
- 507 41. Rueda, N.; Santos, J.C.S. dos; Torres, R.; Ortiz, C.; Barbosa, O.; Fernandez-Lafuente, R. Improved
508 performance of lipases immobilized on heterofunctional octyl-glyoxyl agarose beads. *RSC Adv.* **2015**, *5*,
509 11212–11222, doi:10.1039/C4RA13338B.
- 510 42. Santos, J.C.S. dos; Rueda, N.; Sanchez, A.; Villalonga, R.; Gonçalves, L.R.B.; Fernandez-Lafuente, R.
511 Versatility of divinylsulfone supports permits the tuning of CALB properties during its immobilization.
512 *RSC Adv.* **2015**, *5*, 35801–35810, doi:10.1039/C5RA03798K.
- 513 43. Secundo, F.; Carrea, G.; Soregaroli, C.; Varinelli, D.; Morrone, R. Activity of different *Candida antarctica*
514 lipase B formulations in organic solvents. *Biotechnology and Bioengineering* **2001**, *73*, 157–163,
515 doi:10.1002/bit.1047.
- 516 44. Chamouleau, F.; Coulon, D.; Girardin, M.; Ghoul, M. Influence of water activity and water content on
517 sugar esters lipase-catalyzed synthesis in organic media. *Journal of Molecular Catalysis B: Enzymatic* **2001**,
518 *11*, 949–954, doi:10.1016/S1381-1177(00)00166-1.
- 519 45. Yadav, G.D.; Lathi, P.S. Kinetics and mechanism of synthesis of butyl isobutyrate over immobilised
520 lipases. *Biochemical Engineering Journal* **2003**, *16*, 245–252, doi:10.1016/S1369-703X(03)00026-3.
- 521 46. Zhao, H.; Nathaniel, G.A.; Merenini, P.C. Enzymatic ring-opening polymerization (ROP) of lactides and
522 lactone in ionic liquids and organic solvents: digging the controlling factors. *RSC Adv.* **2017**, *7*, 48639–
523 48648, doi:10.1039/C7RA09038B.
- 524 47. Mei, Y.; Kumar, A.; Gross, R. Kinetics and Mechanism of *Candida antarctica* Lipase B Catalyzed Solution
525 Polymerization of ϵ -Caprolactone. *Macromolecules* **2003**, *36*, 5530–5536, doi:10.1021/ma025741u.
526



© 2020 by the authors. Submitted for possible open access publication under the terms and conditions of the Creative Commons Attribution (CC BY) license (<http://creativecommons.org/licenses/by/4.0/>).